

RESEARCH

Open Access



Cyclic Loading Test of Structural Walls with Small Openings

Hyun-Jin Yu¹, Su-Min Kang^{1*}, Hong-Gun Park² and Lan Chung³

Abstract

This study aimed to investigate the effects of small openings on the structural performance of reinforced-concrete (RC) structural walls. Cyclic lateral loading tests were conducted on five RC walls with an aspect ratio of 2.6 and small openings. The main test parameter was the size of the small openings. The specimens were designed to fail after flexural yielding, considering the typical failure mode of slender RC walls. The structural performances of the test specimens were analyzed based on the test results in terms of the load-carrying capacity (flexural strength), hysteretic behavior, strain distribution, and the size of the openings. The specimens showed flexural yielding regardless of the size of the openings, and the flexural strength and deformation capacity were not significantly affected by the small openings. This result indicates that small openings do not affect the flexural behavior of slender walls if the walls have sufficient shear resistance and the small openings are located away from the extreme compressive end and in the compression zone where compressive stress does not decrease.

Keywords: RC structural walls, small openings, flexural strength, strain distribution, cyclic loading test

1 Introduction

Reinforced concrete (RC) structural walls play an important structural role in high-rise apartment buildings because they support considerable gravity loads and lateral loads. These RC structural walls feature various types of openings, such as small openings for machine and electric boxes, medium openings for water pumps, and large openings for windows and doors, as shown in Fig. 1. However, the effects of such small openings on the structural performance of RC structural walls have been rarely studied. Various experimental and analytical studies have been carried out on RC structural walls with openings. Nevertheless, existing studies mainly focused on walls with relatively large and perforated openings. Massone et al. (2019b) investigated the cyclic response of RC walls with relatively large openings through experimental tests and numerical analysis. Massone et al. (2019a) experimentally investigated the cyclic response of RC walls with setback discontinuities. Taylor et al. (1998) studied

the design of slender reinforced concrete walls with perforated and large openings. Ali and Wight (1990) investigated reinforced concrete structural walls with staggered opening configurations under reversed cyclic loading.

Furthermore, there are no clear application criteria for reinforcement on openings of RC structural walls in concrete structure standards, such as American Concrete Institute Committee 318 (ACI 2011), Korea Concrete Institute 2012 (KCI 2012), and Korean Building Code (KBC) 2016 (AIK 2016). In the structural analysis of reinforced concrete walls, only large openings are considered, whereas medium and small openings are minimally considered and excessive reinforcement details are applied collectively.

However, as many openings have small sizes and only partially penetrate the thickness direction, the openings are not expected to have significant effects on the structural behavior of structural walls. Therefore, collective application of reinforcement on the openings of structural walls appears to be an uneconomical measure that unnecessarily increases the amount of re-bar and decreases the workability of wall construction.

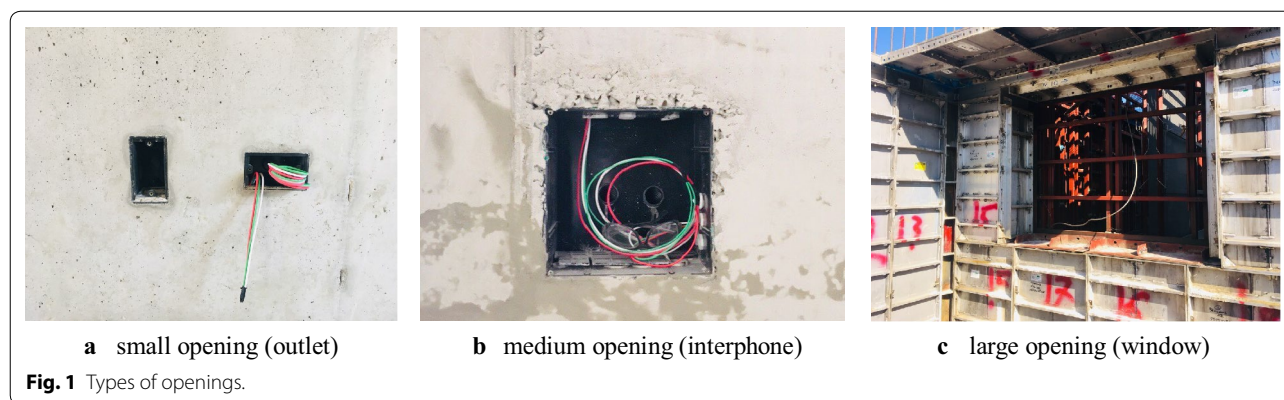
In this study, the structural performance of RC structural walls with relatively small and unpenetrated

*Correspondence: kangsm@cbnu.ac.kr

¹ Department of Architectural Engineering, Chungbuk National University, Cheong-Ju 28644, Republic of Korea

Full list of author information is available at the end of the article

Journal information: ISSN 1976-0485 / eISSN 2234-1315



openings was investigated. A cyclic lateral loading test was conducted on one control RC wall specimen without opening and four RC wall specimens with openings to verify the performance of RC structural walls with various small openings. The test results were analyzed based on the strain of steel re-bars. Through this experiment, the influence of small openings on the structural performance of the RC structural walls was experimentally investigated, and the structural safety of RC structural walls with small openings could be stably achieved based on their ultimate behavior.

2 Test Plan

2.1 Structural Characteristics of RC Walls and Types of Openings in the Walls of Apartment Buildings

The structural characteristics and types of openings of RC structural walls in high-rise apartment buildings in Korea were analyzed to determine the test variables. Figures 2 and 3 show typical structural plans of two high-rise apartment buildings in Korea. In general, the structural RC walls used for the high-rise apartment buildings are very long and deformed with connected cross sections (Figs. 2, 3). In such deformed or long walls, small-sized openings are considered less likely to affect the performance of the structural RC wall owing to the relatively small reduction in the sectional area. Therefore, structural characteristics, such as wall length, wall thickness, wall height, vertical/horizontal ratio of re-bar, and axial compressive load ratio, were analyzed for a single wall with relatively small length, as shown by the red solid line in Figs. 2 and 3, rather than deformed walls or long walls.

From the analysis of the re-bar ratio, compressive load ratio, and failure mode for single walls with relatively small length (Figs. 2, 3), the wall length, wall thickness, wall height, vertical re-bar ratio, and horizontal re-bar ratio were determined as 700–1200 mm, 180–250 mm, 56,000–70,000 mm, 0.15–0.84%, and 0.16–0.46%, respectively. In the case of the axial compressive load ratio at the bottom of the wall at the service load state, 5–13% of

the compressive strength of the entire wall section was loaded ($P = 0.05 - 0.13A_g f'_c$, where A_g is the total area of the wall section, f'_c is the compressive strength of concrete); therefore, approximately 10% of the compressive strength was loaded on average ($P_{aver} = 0.10A_g f'_c$). In case of failure mode, assuming that the lateral force acts as inverse triangular distribution load to the RC walls, flexural failure is expected rather than brittle shear failure because the shear performance of the wall is superior to the load that causes flexural failure.

In order to investigate the size of the opening, which is the main test variable, the types of openings occurring in the RC structure wall of the apartment were classified. Table 1 presents a summary of the sizes, showing that most of the openings in the wall were less than 350 mm × 400 mm (width × length) in area, with a thickness less than half of the wall thickness.

2.2 Test Variables and Specimen Details

As shown in Fig. 4, five RC wall specimens (Specimens A–E) were fabricated; the width, thickness, height, and aspect ratio (wall height to wall width ratio) of the specimens are 1200 mm, 180 mm, 3125 mm, and 2.6, respectively. The lower base of the specimens was reinforced with 2.26% (22-D29) flexural reinforcement and 0.37% (24-D22) shear reinforcement, whereas the upper loading beam was reinforced with 1.62% (8-D25) flexural reinforcement and 0.19% (10-D16) shear reinforcement to prevent damage to the lower base and the upper loading beam before wall failure. The shear strength corresponding to flexural strength (V_f) was designed to be approximately half of the shear performance of the wall ($V_n = V_c + V_s$, where V_c is the shear strength of concrete and V_s is the shear strength of shear reinforcement) to induce flexural failure of the wall specimens because as mentioned above, failure of RC structural walls in high-rise apartment buildings is expected to be due to flexural failure. The shear strength corresponding to the flexural strength (V_f) was calculated by dividing the moment

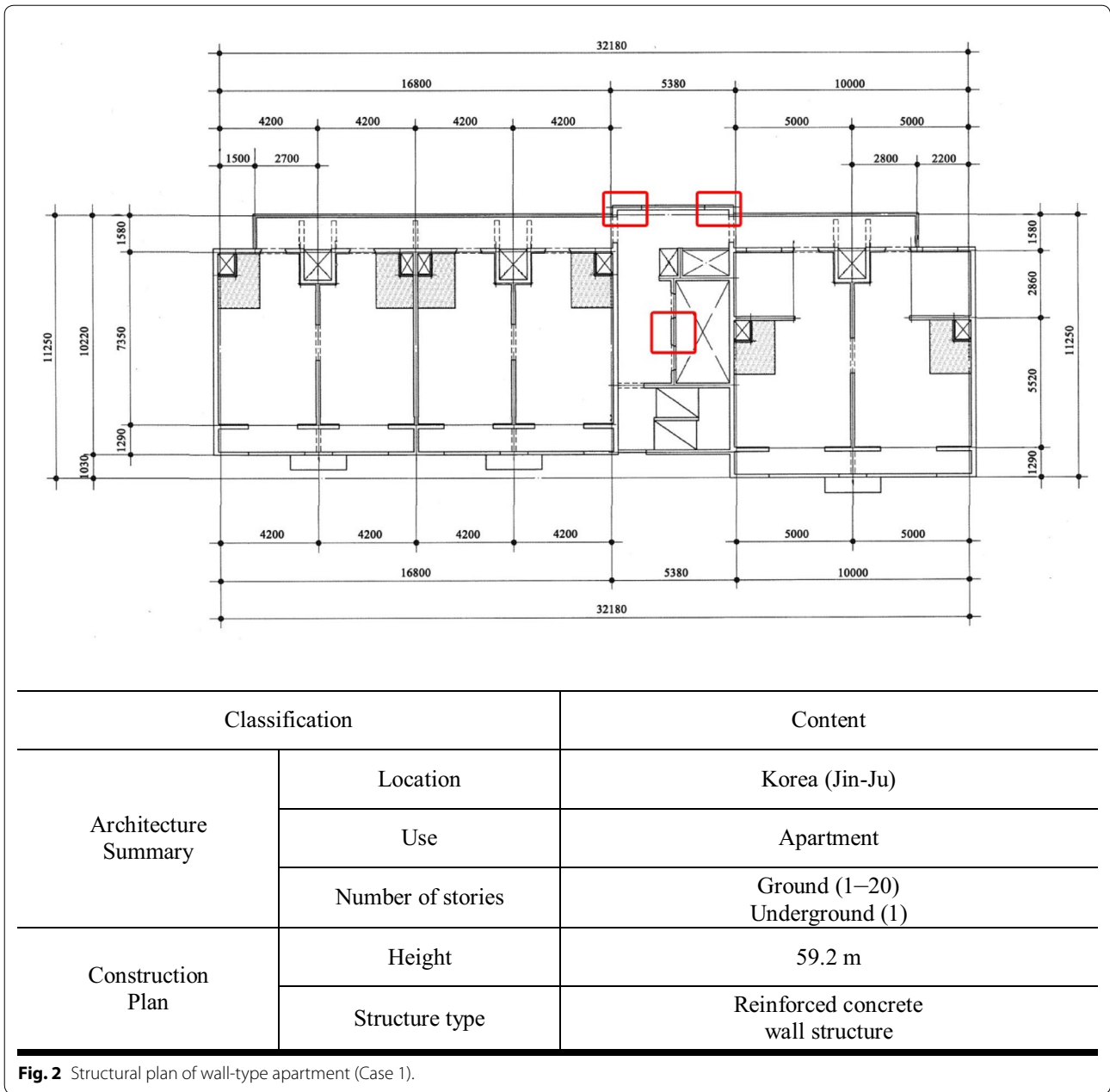


Fig. 2 Structural plan of wall-type apartment (Case 1).

strength of the wall (M_n) by the wall height (h). Furthermore, the shear strength of concrete (V_c) and shear strength of shear reinforcement (V_s) were determined using Eqs. (1)–(2)

$$V_c = 0.28\sqrt{f'_c}hd + \frac{N_u d}{4l_w} \quad (\text{N, MPa, mm}) \quad (1a)$$

$$V_c = \left[0.05\sqrt{f'_c} + \frac{l_w(0.10\sqrt{f_{ck}} + 0.2\frac{N_u}{l_w t})}{\frac{M_u}{V_u} - \frac{l_w}{2}} \right] hd \quad (\text{N, MPa, mm}) \quad (1b)$$

$$V_s = \frac{A_{vh}f_y h d}{s_h} \quad (\text{N, MPa, mm}) \quad (2)$$

where the shear strength of concrete (V_c) is defined as the smaller of the values calculated in Eqs. (1a) and (1b), f'_c is the compressive strength of concrete (MPa), N_u is the axial load, l_w is the wall length (mm), t is the wall thickness (mm), d is the effective width of the wall ($=0.8 l_w$, mm), V_u and M_u are the shear force and flexural moment at the critical section, A_{vh} is the cross-sectional area of the shear reinforcement (mm^2), s_h

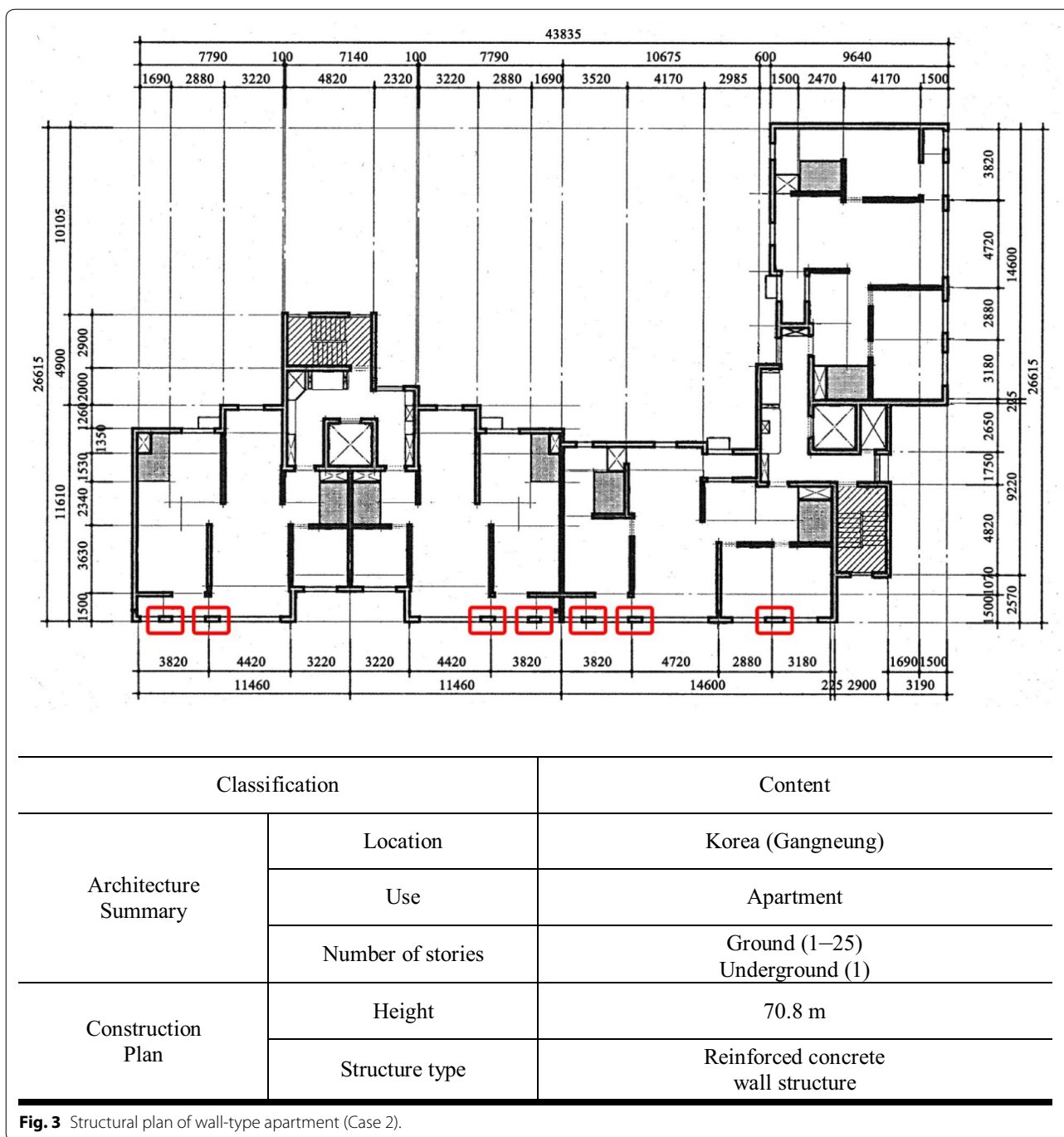


Fig. 3 Structural plan of wall-type apartment (Case 2).

is the spacing of the shear reinforcement (mm), and f_{yh} is the yield strength (MPa) of the shear reinforcement. The horizontal shear reinforcement spacing of the specimens was designed to be 200 mm, which is the minimum value of $3t$, 450 mm, and $l_w/5$. In this case, the horizontal shear reinforcement at the opening portion of Specimens (B–E) might be cut off; therefore, to prevent this, the horizontal shear reinforcement at the opening

portion was moved upward. The vertical flexural reinforcement was placed at 50 mm, 455 mm, 745 mm, and 1150 mm from the wall boundary, considering the location of the openings (Fig. 4). The opening sizes of each specimen were determined based on the results of analysis presented in Table 1 as the main experimental variables. The sizes of openings (width × length × thickness, mm) of each specimen are as follows: Specimen A-no

Table 1 Types of small openings.

Type	Usage	Opening size (width × length × thickness, mm)	Location of wall	
Electricity A	Wall box CSW5	274 × 117 × 54	Inner wall	
	Wall box CSW4	225 × 117 × 54	Inner wall	
	Wall box CSW3	182 × 117 × 54	Inner wall	
	Wall box CSW2	136 × 117 × 54	Inner wall	
	Wall box CSW1	68 × 117 × 54	Inner wall	
	Video phone	350 × 262 × 80	Inner wall	
	LP-1 panel PB	150 × 150 × 100	External wall	
	LP-1 panel PB	150 × 150 × 100	External wall	
	Sub panel PB	150 × 150 × 100	External wall	
	Door lock	100 × 100 × 54	External wall	
Electricity B	LM/LEM panel PB	300 × 300 × 200	External wall	
	Wall box CSW5	274 × 117 × 54	Inner wall	
	Wall box CSW4	225 × 117 × 54	Inner wall	
	Wall box CSW3	182 × 117 × 54	Inner wall	
	Wall box CSW2	136 × 117 × 54	Inner wall	
	Wall box CSW1	68 × 117 × 54	Inner wall	
	LP-1 panel PB	150 × 150 × 100	External wall	
	LP-1 panel PB	150 × 150 × 100	External wall	
	Machine	A/C box	240 × 260 × 80	External wall
		A/C box	135 × 400 × 80	External wall

openings, Specimen B-150 mm × 120 mm × 60 mm, Specimen C-250 mm × 250 mm × 90 mm, Specimen D-300 mm × 300 mm × 90 mm, Specimen E-300 mm × 300 mm × 90 mm + reinforced openings. The vertical and horizontal positions of the openings in each specimen are shown in Fig. 4, which are determined considering the actual location of the small openings in each floor.

The specimens were designed by assuming the yield strength of vertical flexural reinforcement (f_y) = 500 MPa, the yield strength of horizontal shear reinforcement (f_{yh}) = 400 MPa, the compressive strength of concrete (f'_c) = 30 MPa, and an axial force of $0.15 A_g f_{ck}$. The actual strength of concrete and reinforcing bar was measured as the mean value of the material test results on the day of testing. The actual yield strength of vertical flexural reinforcement (f_y), actual yield strength of horizontal shear reinforcement (f_{yh}), and actual compressive strength of concrete (f'_c) were found to be 661–674 MPa, 494–512 MPa, 30.7–31.7 MPa, respectively, as summarized in Table 2 (Korea Standards Association 2008, 2010).

2.3 Test Set-up, Loading Plan, and Measurement Plan

The experiments were carried out using the test setup shown in Fig. 5. A constant axial load was applied to the specimens through two hydraulic actuators ($P = 0.15 A_g f_{ck}$) until the end of the test. The lateral

cyclic load was repeatedly applied to the upper beam of the specimen using a displacement controlled actuator. Although not shown in Fig. 5b, a guide steel frame was installed at approximately 1/3 height (1600 mm from the strong floor) and 2/3 height (2700 mm from the strong floor) of the wall specimen to prevent out-of-plane buckling of the test specimen.

The lateral load was applied to satisfy the displacement ratio (Δ/H), as shown in Fig. 6, according to the ACI 374 test guideline (ACI 2013). Here, Δ is the displacement of the upper beam at lateral loading and H is the height of the wall. To prevent sudden deformation of the specimen, the lateral load was applied at 0.25 Δ/H intervals up to a displacement ratio of 1.0 Δ/H , then, the test was repeated at intervals of 0.5 Δ/H , 1.0 Δ/H , and 1.5 Δ/H . The test was stopped when the strength of the specimen decreased to 70% or less after the maximum strength or sudden load reduction occurred due to specimen failure. As shown in Fig. 7, linear variable differential transformers (LVDTs) were used to measure the total lateral displacement (L1), shear deformation (L2–L5), wall-based slip deformation (L6), flexural deformation (L7–L14), and foundation horizontal slip deformation (L base). Strain gauges were attached to the flexural reinforcement and horizontal shear reinforcement at the lower part of the wall where considerable deformations are expected to occur.

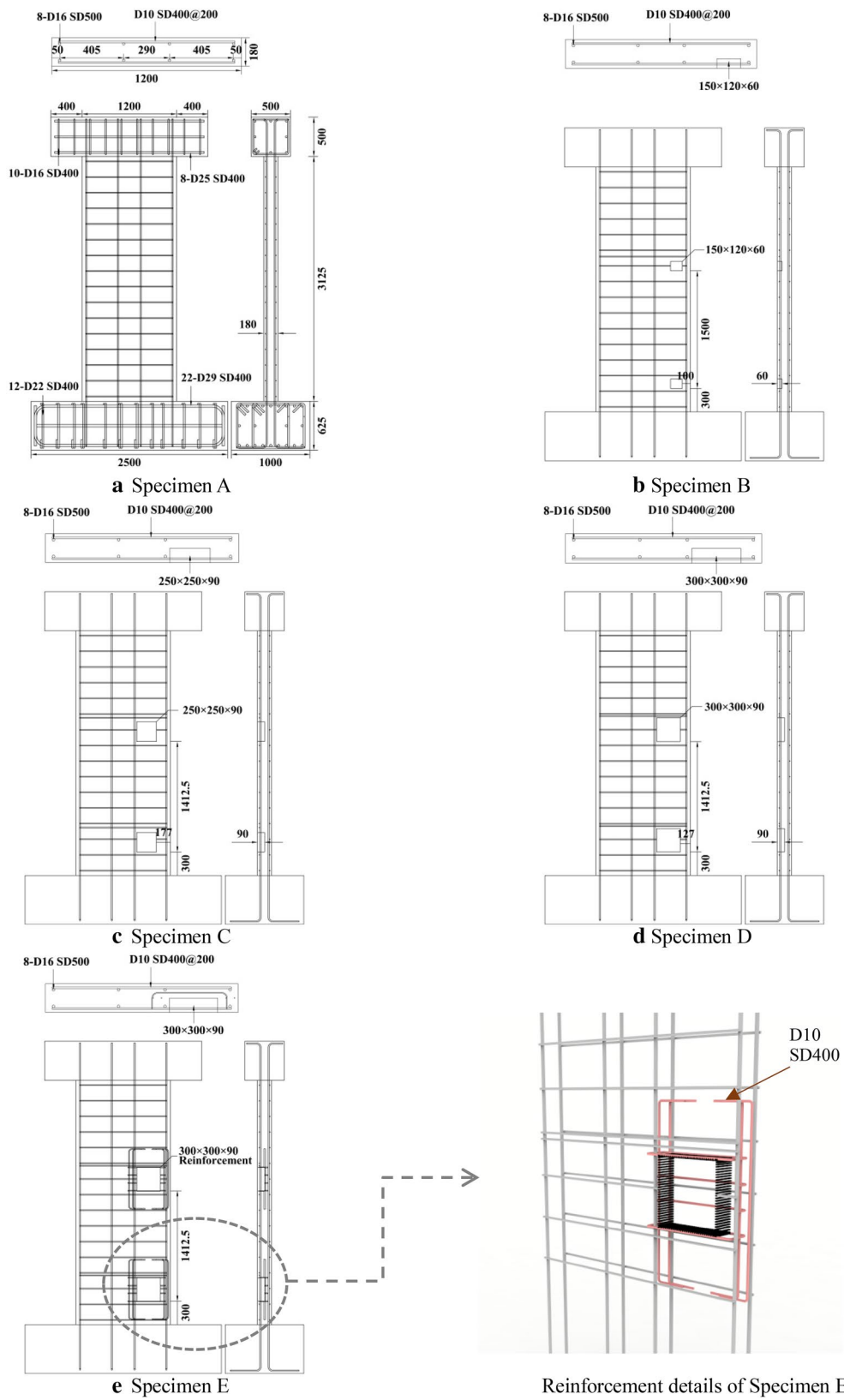


Fig. 4 Details of test specimens.

Table 2 Material properties and main parameters of test specimens.

Specimen	Failure mode	f_{ck}^a (MPa)	$P/f_{ck}A_g^b$	Horizontal shear re-bars (D10)		Flexural re-bars (D16)		Main parameter (opening size: width x length x thickness, mm)
				f_{yh} (MPa)	ρ_h (%)	f_{yv} (MPa)	ρ_h (%)	
A	Flexural yielding	30.7	0.15	512	0.004	666	0.0074	–
B		30.7	0.15	494	0.004	661	0.0074	150 × 120 × 60
C		30.7	0.15	499	0.004	669	0.0074	250 × 250 × 90
D		31.7	0.15	497	0.004	674	0.0074	300 × 300 × 90
E		31.7	0.15	495	0.004	671	0.0074	300 × 300 × 90 Reinforcement

^a Compressive strength test results of experimental data.

^b Ratio of axial force applied to the specimen section; f_{ck} is compressive strength test results of experimental data.

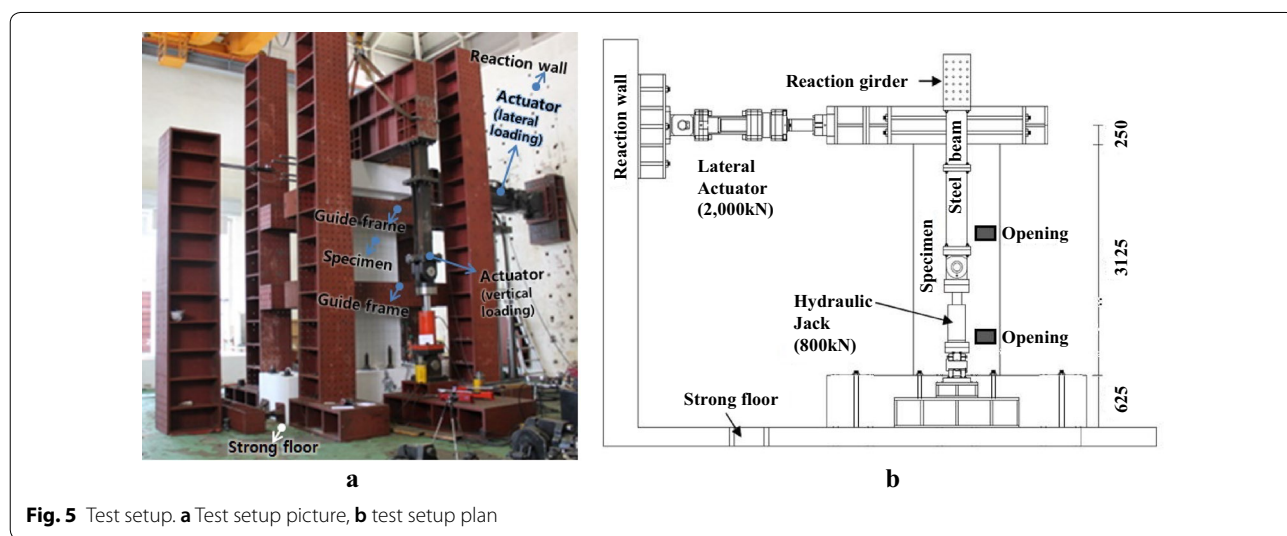


Fig. 5 Test setup. **a** Test setup picture, **b** test setup plan

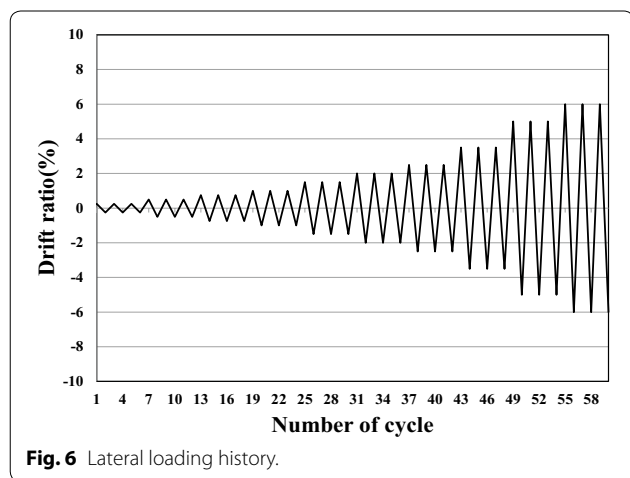


Fig. 6 Lateral loading history.

3 Test Results

3.1 Lateral Load–Drift Ratio Relation

Figure 8 shows the relationship between the lateral load (measured at the loading actuator) and the drift ratio (Δ/H) for each specimen. The shear strength corresponding to the flexural strength (V_f), which was calculated based on the material test results, maximum test strength (V_{test}), ultimate displacement (δ_u), displacement at the maximum strength (δ_m), and initial stiffness of each specimen (K_i) are presented in Fig. 8 and Table 3. The ultimate displacement (δ_u) is the displacement when the load carrying capacity is decreased to 75% of the maximum strength.

The experimental results show that all the specimens have higher load carrying capacity (V_{test}) than the load

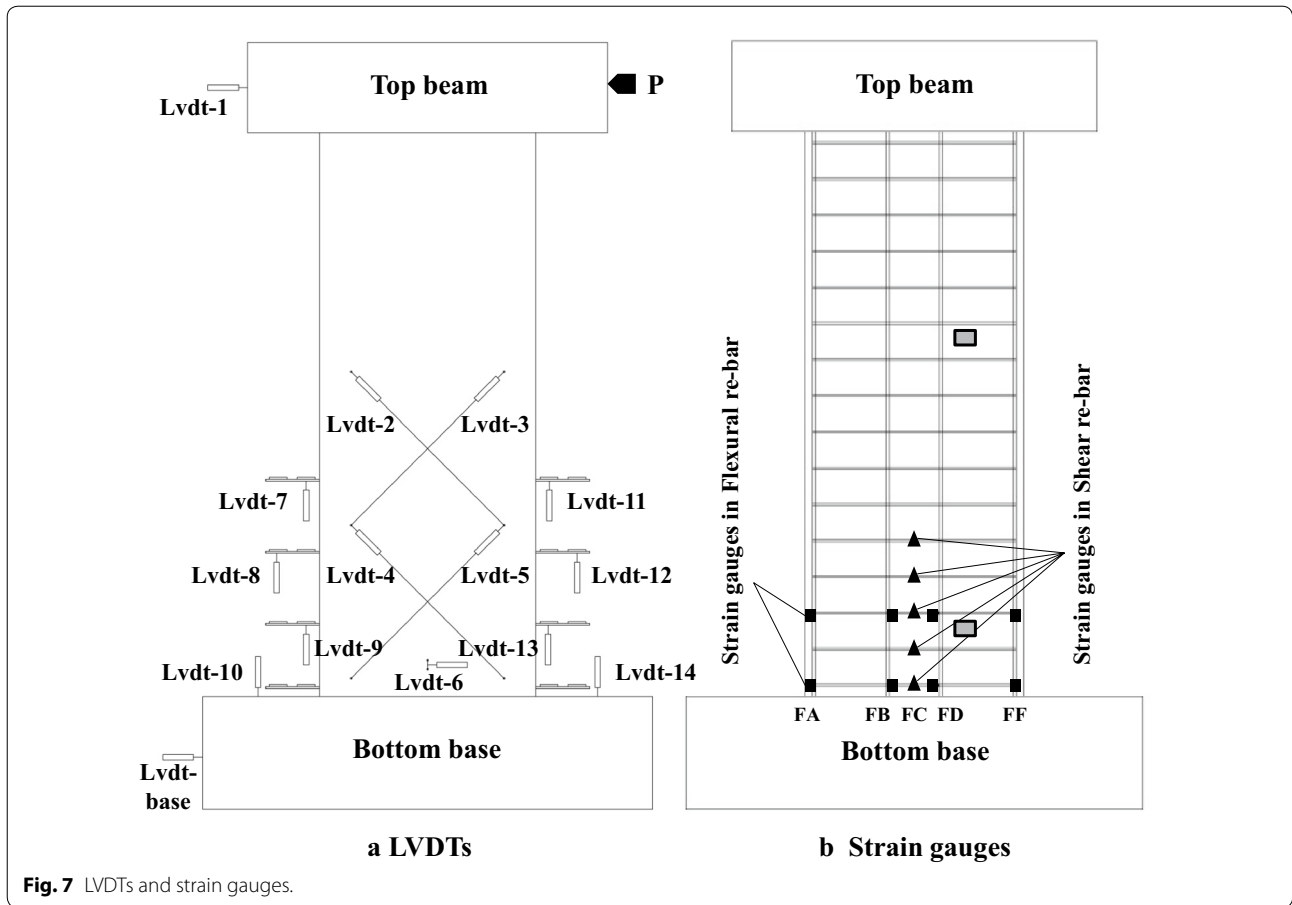


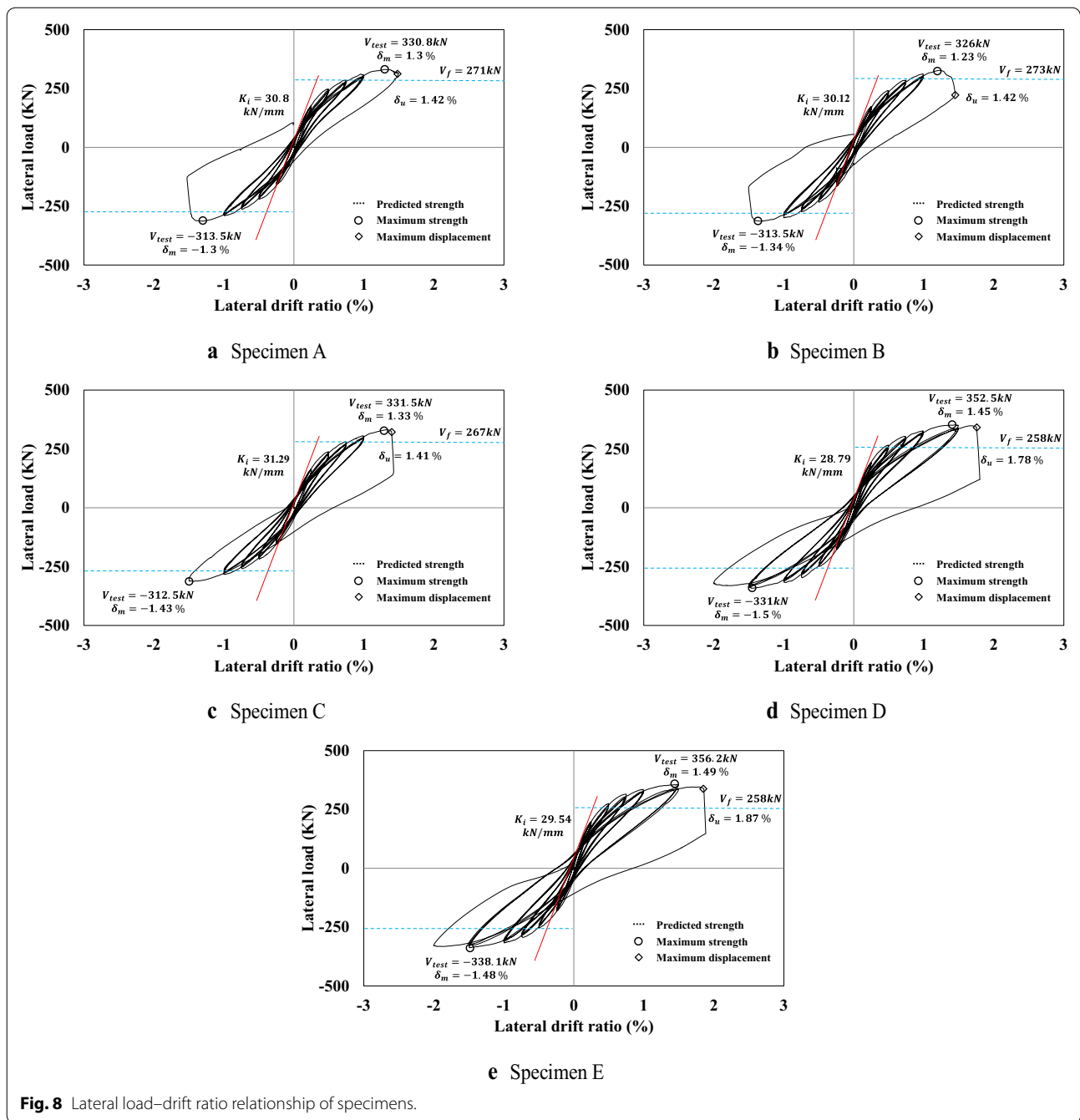
Fig. 7 LVDTs and strain gauges.

corresponding to the predicted flexural strength (V_f) regardless of the size of the openings and the specimens exhibited ductile behavior after flexural yielding (Fig. 8). The predicted flexural strength (V_f) for each specimen in Table 3 was calculated as follows. The first predicted strength ($V_{f(1)} = M_{n[base]}/h$) was calculated based on the flexural moment strength without opening ($M_{n[base]}$) and the total height ($h = 3.375$ m) as there is no opening at the bottom of the wall. In addition, the second predicted strength ($V_{f(2)} = M_{n[opening]}/h'$) was calculated based on the flexural strength ($M_{n[opening]}$) at the wall section where the opening is located and the height from the lowest wall section with opening to the loading point ($h' = 3.075$ m) as flexural failure can occur at the location of the opening. Therefore, the final predicted strength (V_f) was determined as the lesser of $V_{f(1)}$ and $V_{f(2)}$, and the expected failure location of the specimen was also determined as the region where the final predicted strength occurs (see Table 3).

It is noteworthy that all the specimens were planned to have identical concrete compressive strength, rebar ratio, yield strength, and axial force but different sizes of openings. The control Specimen A without openings and the

remaining Specimens B–E with various openings exhibited similar structural performance in terms of maximum test strength (V_{test}), ultimate displacement (δ_u), displacement at maximum strength (δ_m), and initial stiffness of each specimen (K_i) (Fig. 8). The maximum strength, initial stiffness, and ultimate displacement of Specimen A were 330.8 kN, 30.8 kN/mm, and 1.42%, respectively. For Specimens B–E, the values of the maximum strength were 326 kN, 331.5 kN, 352.5 kN, and 356.2 kN, the initial stiffness were 30.12 kN/mm, 31.29 kN/mm, 28.79 kN/mm, and 29.54 kN/mm, and the ultimate displacement were 1.42%, 1.41%, 1.78% and 1.87%, respectively, which are somewhat greater or similar to those of Specimen A. For all the specimens, the ratio of the experimental maximum strength (V_{test}) to the expected strength (V_f) was 1.19–1.38, suggesting that the five specimens have sufficient strength.

According to Table 3, because the opening of Specimen B is very small, failure is expected to occur at the base of the wall of Specimen B similar to Specimen A with no opening. On the other hand, the failures of Specimens C, D, and E are expected to occur at the region where the opening is located because these specimens have



relatively large openings. Figure 9 shows the failure pattern at the end of the test; the failure location of Specimen B is closer to the wall base, and those of Specimens C, D, and E are higher than that of Specimen B.

Change in the failure location can affect the structural performance of Specimens D and E with relatively large openings, which exhibited higher strength and deformation than expected. In addition, it is considered that the strength and deformability of Specimens D and E with

relatively large openings are higher than those of control Specimen A partly due to the difference in the behavior of the reinforcing bars in each specimen. Figure 10 shows the tensile stress–strain relationship of the flexural rebar (D16) used in Specimens A, D, and E. As shown in the figure, the tensile hardening behavior of the reinforcing bars used in Specimens D and E starts earlier than that of the reinforcing bar used in Specimen A. It was also found that the tensile stress of the reinforcing bars used in

Table 3 Test results.

Specimen	$V_{f(1)}$ ^a (kN)	$V_{f(2)}$ ^b (kN)	Expected failure location	V_f ^c (kN)	V_n ($V_c + V_s$) (kN)	K_i (kN/mm)	V_{test} (kN)	δ_m ^d (%)	δ_u ^e (%)	$\frac{V_{test}}{V_f}$
A	271	–	Wall base	271	510	30.8	330.8	1.3	1.42	1.22
B	273	279	Wall base	273	498	30.12	326	1.23	1.42	1.19
C	272	267	Opening	267	502	31.29	331.5	1.33	1.41	1.24
D	278	258	Opening	258	503	28.79	352.5	1.45	1.78	1.37
E	279	258	Opening	258	502	29.54	356.2	1.49	1.87	1.38

^a $V_{f(1)} = M_{n[base]}/h$, where $M_{n[base]}$ =nominal moment strength at wall base, h =height from wall base (3.375 m).

^b $V_{f(2)} = M_{n[opening]}/h'$, where $M_{n[opening]}$ =nominal moment strength at opening, h' =height from the lowest opening (3.075 m).

^c $V_f = \text{thelesserof } V_{f(1)} \text{ and } V_{f(2)}$.

^d Displacement ratio at maximum strength.

^e Displacement ratio when the specimen reached 70% of the maximum strength after the maximum strength.

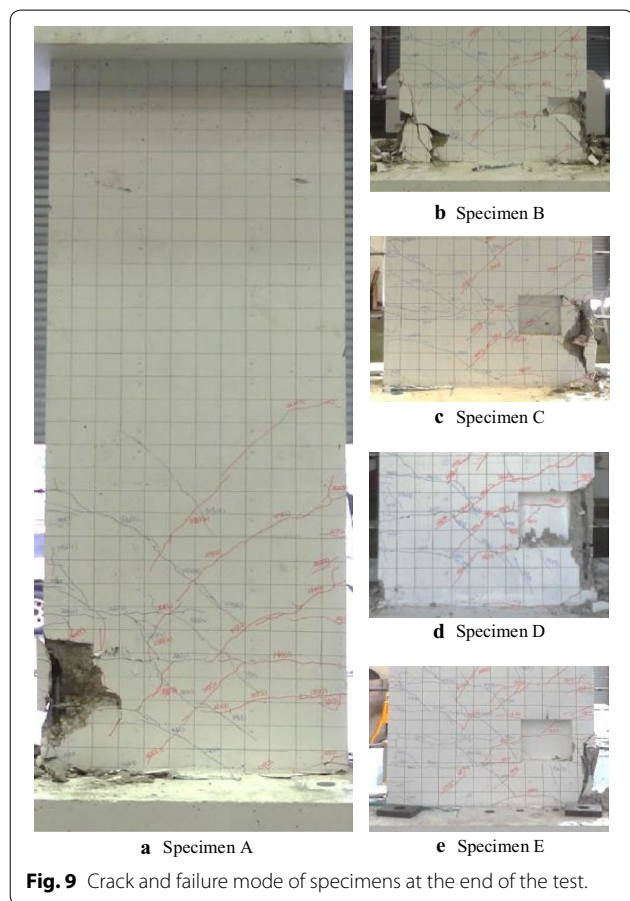


Fig. 9 Crack and failure mode of specimens at the end of the test.

Specimens D and E is approximately 4% larger than that of the reinforcing bar used in Specimen A at a strain of 0.015 at which the ultimate behavior of the specimen occurred since the maximum strain of the flexural re-bar during the test was in the range of 0.015–0.020, as shown in Fig. 11.

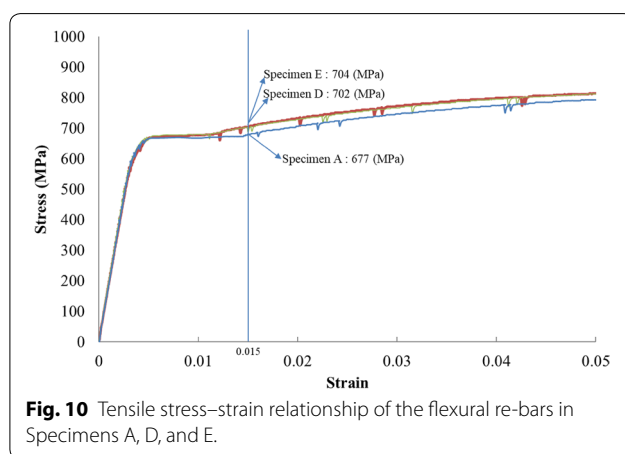


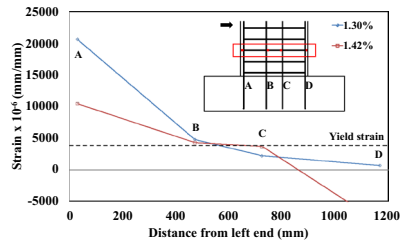
Fig. 10 Tensile stress–strain relationship of the flexural re-bars in Specimens A, D, and E.

Therefore, it is considered that Specimens D and E with relatively large openings exhibited slightly better structural performance than the control Specimen A, contrary to general expectation, due to the difference between the tensile behavior of the reinforcing re-bars and the change in the failure location.

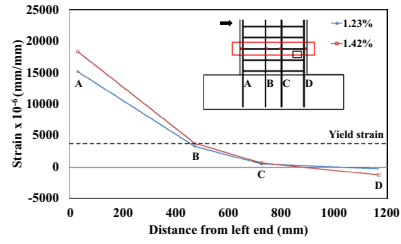
3.2 Crack Pattern and Failure Mode

Figure 9 shows the crack and failure patterns of the test specimen after the experiment. Initial flexural cracks and horizontal cracks occurred at the boundary of all specimens at a displacement ratio of approximately 0.25%. Diagonal cracks occurred in the lower part of the wall at displacement ratios of 0.47–0.68%.

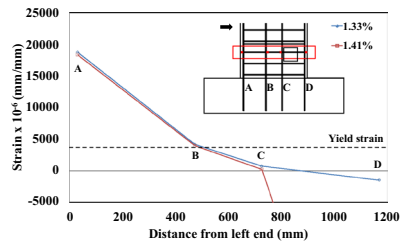
At a displacement ratio of 0.7%, flexural and diagonal cracks in the control specimen increased in the web and the lower part of the wall, the boundary concretes were damaged after yielding of the flexural reinforcement, and the experiment was completed with



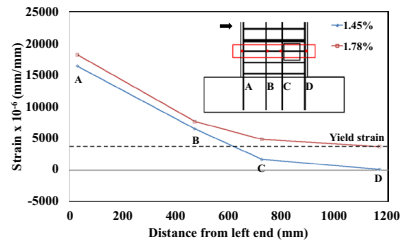
(A) Specimen A



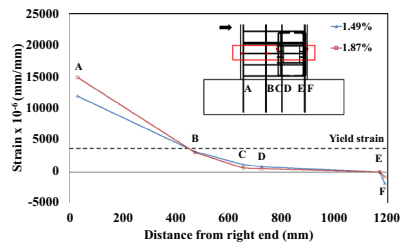
(B) Specimen B



(C) Specimen C

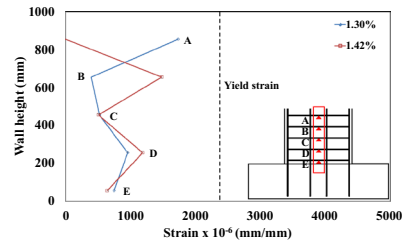


(D) Specimen D

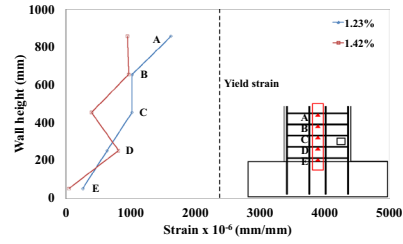


(E) Specimen E

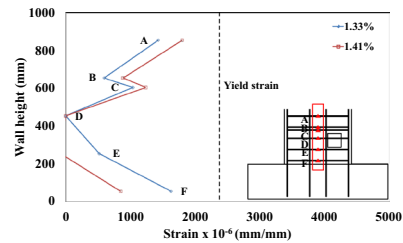
a Strain distribution of vertical re-bars



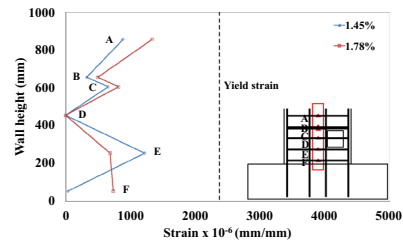
(A) Specimen A



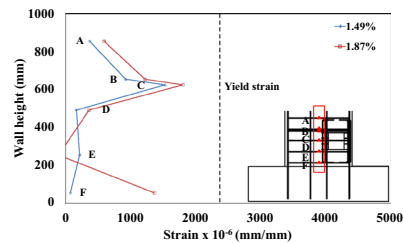
(B) Specimen B



(C) Specimen C



(D) Specimen D



(E) Specimen E

b Strain distribution of horizontal re-bars

Fig. 11 Strain distribution in horizontal and vertical reinforcements.

crushing of the compressive concrete and buckling of the exposed flexural reinforcement at a displacement ratio of 1.45%. In Specimens B and C with relatively small openings, flexural and diagonal cracks increased at displacement ratios of 0.81% and 0.72%, respectively in the web and the lower part of the wall, and the experiment was completed with crushing of the compressive concrete and buckling of the outermost reinforcing bars at displacement ratios of 1.45% and 1.42%, respectively. In Specimens D and E with larger openings, flexural and diagonal cracks increased at displacement ratios of 0.75% and 0.72%, respectively in the web and the lower part of the wall, and the experiment was completed with crushing of the compressive concrete and buckling of the outermost reinforcing bars at displacement ratios of 1.79% and 1.87%, respectively. As mentioned above (and shown in Fig. 9), the failure location of Specimen B is closer to the wall base, whereas those of Specimens C, D, and E are higher than that of Specimen B owing to the difference in the opening size. However, although each specimen had a different opening size, they showed similar cracking and failure characteristics.

3.3 Strain of Re-bars

Figure 11a shows the strain distributions of the vertical flexural bars placed along the wall width direction, whereas Fig. 11b shows the strain distribution of the horizontal shear bars along the wall height direction, obtained from the steel strain gauge shown in Fig. 7b.

The flexural reinforcement of all specimens showed a large strain after yielding (Fig. 11a). In the ultimate behavior of the specimen, the vertical flexural re-bar at the tensional edge showed a large strain of 0.015–0.020 irrespective of the presence of openings, size of the openings, and reinforcement of the openings (Fig. 11a). All the horizontal shear reinforcements did not yield until the final failure, no significant shear damage occurred, and no significant change could be attributed to the size of the openings (Fig. 11b). This means that small openings

do not significantly affect the ultimate behavior of flexure-dominated walls.

3.4 Strength According to Opening Location and Size

Table 4 presents the predicted nominal strengths (M_n), test strengths (M_u), and strength ratios of M_u and M_n according to the size and location of the openings. The nominal strengths (M_n) of Specimens A–E under the Bernoulli–Euler hypothesis were calculated as 916 kN m, 920 kN m, 820 kN m, 794 kN m, and 793 kN m, respectively. However, their test strengths (M_u) were 1116.45 kN m, 1100.25 kN m, 1019.36 kN m, 1083.9 kN m, and 1095.31 kN m, respectively. Therefore, the test strengths (M_u) of Specimens A–E are 22%, 20%, 24%, 37%, and 38% larger than their nominal strengths (M_n).

Figure 12 shows the nominal strength, length of the compression zone, and location of the openings of each specimen at the critical section in the ultimate state, which can be obtained through cross section analysis considering the openings of the walls and the left concrete of the unpenetrated opening based on the Bernoulli–Euler hypothesis. Although the openings of test

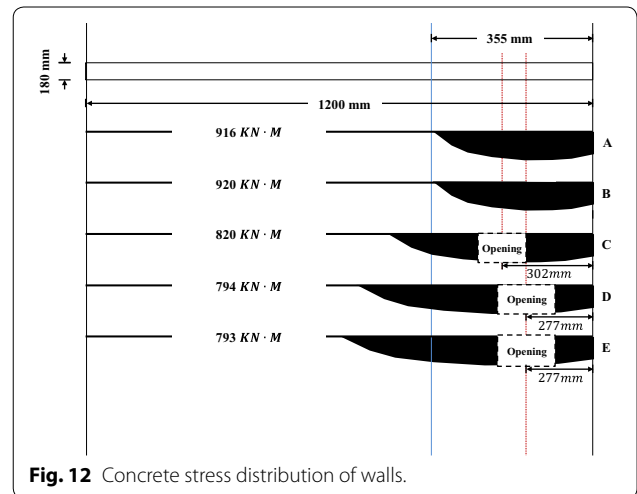


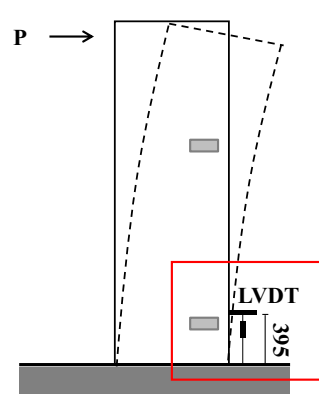
Fig. 12 Concrete stress distribution of walls.

Table 4 Analysis of test results.

Specimen	Opening size (mm)	Opening depth (mm)	Opening location from end (m)	Nominal strength M_n (A) at critical section (kN m)	Test results		Strength ratio of (B) to (A) (%)
					V_u (kN)	M_u (B) at critical section (kN m)	
A	–	–	–	916	330.8	1116.5	122
B	150 × 120 × 60	60	0.1	920	326	1100.3	120
C	250 × 250 × 90	90	0.177	820	331.5	1019.4	124
D	300 × 300 × 90	90	0.127	794	352.5	1083.9	137
E	300 × 300 × 90 Reinforcement	90	0.127	793	356.2	1095.3	138

Table 5 Ultimate compressive strain at the bottom of the wall.

Specimen	Ultimate compressive strain
B	0.004
C	0.0034
D	0.0038
E	0.0034



Specimens C, D, and E were located in the compression zone, they were not within the region where the compressive stress decreased, but within the region where the compressive stress was stable. Therefore, the flexural behavior or flexural strength of the specimens remained unchanged for various small openings. Based on this, it can be noted that small openings do not affect the flexural behavior of slender walls if the walls exhibit sufficient shear performance and the small openings are located in the compression zone where the compressive stress did not decrease.

However, according to the relationship between the lateral load–drift ratio (Fig. 8), the maximum deformation performance (ultimate displacement ratio of 1.41–1.87%) of each specimen was not sufficient. Furthermore, the final failure of the specimens was due to the damage of concrete through compression (Fig. 9).

To analyze this more precisely, the compressive strain measured by LVDT at the compression end in the lower part of wall at the final failure of the specimens was analyzed, and the results are presented in Table 5 (the compressive strain of Specimen A is not included because of measurement errors). As presented in Table 5, the compressive strain at the compressive end of Specimens B–E ranged from 0.0034 to 0.004. In general, the ultimate compressive strain of a concrete member is an important factor for determining the ductility at flexural failure, and its value varies depending on the stress state of members. The ultimate compressive strain of the flexure-dominated walls had maximum values of 0.004 or less, which are not sufficient or cannot assure sufficient ductility of the wall. These results are similar to those reported in a previous study (Adebar 2013). Therefore, in the case of a slender wall dominated by flexural behavior, it is necessary to secure sufficient ductility of the wall through boundary

confinement at the compressive end of the wall (Thomsen and Wallace 1995; Wallace 1994, 1995).

4 Summary and Conclusion

In this study, five slender RC walls with small openings (one control specimen without openings and four specimens with various openings) were tested under cyclic lateral loading. The primary results of this study are summarized as follows:

1. All specimens exhibited similar behavior regardless of the size and location of the opening. In all specimens, flexural yielding occurred. The test specimens failed by concrete crushing at the compressive end and buckling of the flexural reinforcement. All specimens showed test strengths that were larger than those of the nominal strength by 20–38% and similar deformation capacity.
2. The flexural reinforcement in all specimens showed large strains after yielding irrespective of the presence of openings, size of the openings, and additional reinforcement for the openings. Horizontal shear reinforcements did not yield, and no significant shear damage occurred. This result indicates that small openings did not significantly affect the strength and deformation capacity of the walls.
3. Despite the openings located in the compression zone, the strength in the compression zone was maintained after large deformation. This indicates that the small openings did not significantly affect the flexural behavior of the slender wall if the wall exhibits sufficient shear performance and the small openings are located away from the compression end and in the compression zone where compressive stress does not decrease.

4. The ultimate compressive strain at the compressive end of the specimens in the range of 0.0034–0.004 was not sufficient as compressive strain or could not ensure sufficient ductility of the wall. Therefore, in the case of a slender wall dominated by flexural behavior, securing sufficient ductility of the wall through boundary confinement at the compressive end of the wall is necessary.

The conclusions of this study are from test results using limited specimens. Therefore, additional experimental and analytical studies are necessary to generalize these conclusions under various design conditions.

Acknowledgements

This work was financially supported by the National Research Foundation of Korea (NRF) Grant funded by the Korea Government (MSIT) (No. 2018R1A2B6007559).

Authors' contributions

HJY and SMK carried out the experiments, analyzed the data, and wrote the paper. HGP planned the experiment, determined the test variables, and reviewed the data analyzed by HJY and SMK. LC supervised this project and discussed the overall research such as test plan, test result, and conclusions. All authors read and approved the final manuscript.

Availability of data and materials

Data analyzed in this study are available in the master's thesis of H.J. Yu, Chungbuk National University, 2019.

Competing interests

The authors declare that they have no competing interests.

Author details

¹ Department of Architectural Engineering, Chungbuk National University, Cheong-Ju 28644, Republic of Korea. ² Department of Architecture & Architectural Engineering, Seoul National University, Seoul 08826, Republic of Korea. ³ Department of Architectural Engineering, Dankook University, Yongin 16890, Republic of Korea.

Received: 30 November 2018 Accepted: 6 June 2019

Published online: 22 July 2019

References

- Adebar, P. (2013). Compression failure of thin concrete walls during 2010 Chile earthquake: Lessons for Canadian design practice. *Canadian Journal of Civil Engineering*, 40(8), 711–721.
- Ali, A., Wight, J. K. (1990). *Reinforced concrete structural walls with staggered opening configurations under reversed cyclic loading*. University of Michigan, Report No. UMCE 90-05.
- American Concrete Institute Committee 318. (2011). Building code requirements for structural concrete (ACI 318-11) and Commentary.
- American Concrete Institute Committee 374. (2013). Guide for testing reinforced concrete structural elements under slowly applied simulated seismic loads.
- Architectural Institute of Korea. (2016). Korean Building Code 2016 (KBC 2016).
- Korea Concrete Institute. (2012). Code requirement for reinforced concrete structure Korea Concrete Institute (KCI 2012).
- Korea Standards Association. (2008). KS B 0802:2003 Tensile test method for metallic materials.
- Korea Standards Association. (2010). KS F 2405:2010 Standard test method for compressive strength of concrete.
- Massone, L. M., Diaz, S., Manriquez, I., Rojas, F., & Herrera, R. (2019a). Experimental cyclic response of RC walls with setback discontinuities. *Engineering Structures*, 178, 410–422.
- Massone, L. M., Munoz, G., & Rojas, F. (2019b). Experimental and numerical cyclic response of RC walls with openings. *Engineering Structures*, 178, 318–330.
- Taylor, C. P., Cote, P. A., & Wallace, J. W. (1998). Design of slender reinforced concrete walls with openings. *ACI Structural Journal*, 95, 420–433.
- Thomsen, J. H., Wallace, J. W. (1995). *Displacement-based design of RC structural wall: An experimental investigation of walls with rectangular and T-shaped cross sections*. Department of Civil and Environmental Engineering, Clark University. Report no Cu/Cee-95-06.
- Wallace, J. W. (1994). New methodology for seismic design of reinforced concrete shear walls. *Journal of Structural Engineering ASCE*, 120(3), 863–884.
- Wallace, J. W. (1995). Seismic design of RC structural walls. Part I: New code format. *Journal of Structural Engineering ASCE*, 121(1), 75–87.

Publisher's Note

Springer Nature remains neutral with regard to jurisdictional claims in published maps and institutional affiliations.

Submit your manuscript to a SpringerOpen[®] journal and benefit from:

- Convenient online submission
- Rigorous peer review
- Open access: articles freely available online
- High visibility within the field
- Retaining the copyright to your article

Submit your next manuscript at ► [springeropen.com](https://www.springeropen.com)